

Article

Measurement of Poly(ADP-ribose) Level with Enhanced Slot Blot Assay with Crosslinking

Yuko Kudo ^{1,2}, Yuka Sasaki ^{3,4}, Takae Onodera ^{3,4}, Jun Hashimoto ⁵, Tadashige Nozaki ⁶, Kenji Tamura ⁵, Masatoshi Watanabe ^{2,†}  and Mitsuko Masutani ^{1,3,4,*}

¹ Genome Stability Research Division, Lab of Collaborative Research, National Cancer Center Research Institute, 5-1-1, Tsukiji, Chuo-ku, Tokyo 104-0045, Japan; kudou-yu@kaketsuken.or.jp

² Division of Materials Science & Chemical Engineering, Graduate School of Engineering, Yokohama National University, 79-5, Tokiwadai, Hodogaya-ku, Yokohama 240-8501, Japan; mawata@doc.medic.mie-u.ac.jp

³ Division of Cell Signaling, Lab of Collaborative Research, National Cancer Center Research Institute, 5-1-1, Tsukiji, Chuo-ku, Tokyo 104-0045, Japan; yukasasa@nagasaki-u.ac.jp (Y.S.); takae-o@nagasaki-u.ac.jp (T.O.)

⁴ Department of Frontier Life Sciences, Nagasaki University Graduate School of Biomedical Sciences, 1-7-1 Sakamoto, Nagasaki 852-8588, Japan

⁵ Department of Breast and Medical Oncology, National Cancer Center Hospital, Tsukiji 5-1-1, Chuo-ku, Tokyo 104-0045, Japan; juhashim@ncc.go.jp (J.H.); ketamura@ncc.go.jp (K.T.)

⁶ Department of Pharmacology, Faculty of Dentistry, Osaka Dental University, 8-1, Kuzuhahanazono-cho, Hirakata, Osaka 573-1121, Japan; nozaki@cc.osaka-dent.ac.jp

* Correspondence: mmasutan@nagasaki-u.ac.jp; Tel.: +81-95-819-8502

† Current address: Oncologic Pathology Graduate School of Medicine, Mie University, 2-174 Edobashi, Tsu 514-8507, Japan

Received: 29 March 2018; Accepted: 26 June 2018; Published: 2 July 2018



Abstract: Poly(ADP-ribose) (PAR) formation is catalyzed by poly(ADP-ribose) polymerase (PARP) family proteins in nuclei as well as in cytosols. The anti-PAR antibodies that specifically detect PAR are useful for the quantitative measurement of PAR in cells, in tissue, and in the body. In clinical trials of PARP inhibitors, a pharmacodynamic (PD) assay for the measurement of PARP activity inhibition in peripheral blood mononuclear cells (PBMCs) with dot-blot assay or an ELISA assay using anti-PAR antibodies have been used. In these assays, ex vivo PARP activity and its inhibition assay have been used. For a PD assay to assess the efficacy of the treatment, the measurement of PARP activity inhibition in tumor tissues/cells has been recommended. A dot or slot blot assay may also be suitable for the measurement of such crude tissue samples. Here, we investigate the optimum conditions for a dot/slot blot assay of an ex vivo PARP activity assay by utilizing physical and chemical crosslinking methods. Using 10H monoclonal antibody to PAR, we show that use of a nylon membrane and UV crosslink at 254 nm can stably enhance the detection level of PAR. However, the limitation of this assay is that the size of PAR detectable using the 10H antibody must be around 20 ADP-ribose residues, since the antibody cannot bind PAR of lower size.

Keywords: poly(ADP-ribose); PARP inhibitor; pharmacodynamic assay; UV crosslink

1. Introduction

Poly(ADP-ribose) (PAR) formation is catalyzed by poly(ADP-ribose) polymerase (PARP) family proteins using NAD⁺ as a substrate in nuclei as well as in cytosols. PAR formed in the nuclei and cytoplasm is degraded by poly(ADP-ribose) glycohydrolase (PARG) and ADP-ribosyl hydrolase 3 (ARH3) [1]. The presence of anti-PAR antibodies was reported in the serum of patients suffering from auto-immune diseases [2–4]. Anti-PAR antibodies have also been generated in mice using PAR as an antigen [5]. These anti-PAR antibodies that specifically detect PAR are useful for the quantitative

measurement of PAR in cells and of PAR levels in the tissue and body. Monoclonal antibody 10H is able to specifically recognize PAR [5], and several PAR polyclonal antibodies have become commercially available. Recently, specific PARP inhibitors have been developed and started to be used as anti-cancer agents [6–8]. PARP inhibitors were shown to induce synthetic lethality in cancer cells that harbor gene mutations involved in the loss of the homologous recombination repair of DNA, such as *BRCA1/2* [9,10], *ATM*, *ATR* [11], and *ChIP* [12]. In clinical trials of PARP inhibitors, a pharmacodynamic (PD) assay for the measurement of PARP activity inhibition in peripheral blood mononuclear cells (PBMCs) with dot-blot assay [6] and an NCI advanced protocol [13] ELISA assay using anti-PAR antibodies have been used. In these assays, ex vivo PARP activity and its inhibition level have been measured. For a PD assay, to assess the efficacy of the treatment, the measurement of PARP activity inhibition in tumor tissues/cells has been recommended. For this purpose, a dot or slot blot assay might be more suitable for the quantification in the crude tissue samples. Therefore, we have investigated the optimum conditions for a slot/dot blot assay of ex vivo PARP activity by utilizing physical and chemical crosslinking methods.

2. Results

2.1. Optimization of Slot Blot Assay of PAR Using Crosslinking

A slot/dot blot assay was carried out as reported by Plummer et al. [6]. For the improvement of detection sensitivity, we compared the nylon membrane of Hybond-N and nitrocellulose for slot/dot blot assay. We found that the use of Hybond-N increased the sensitivity of the detection level (Figure 1).

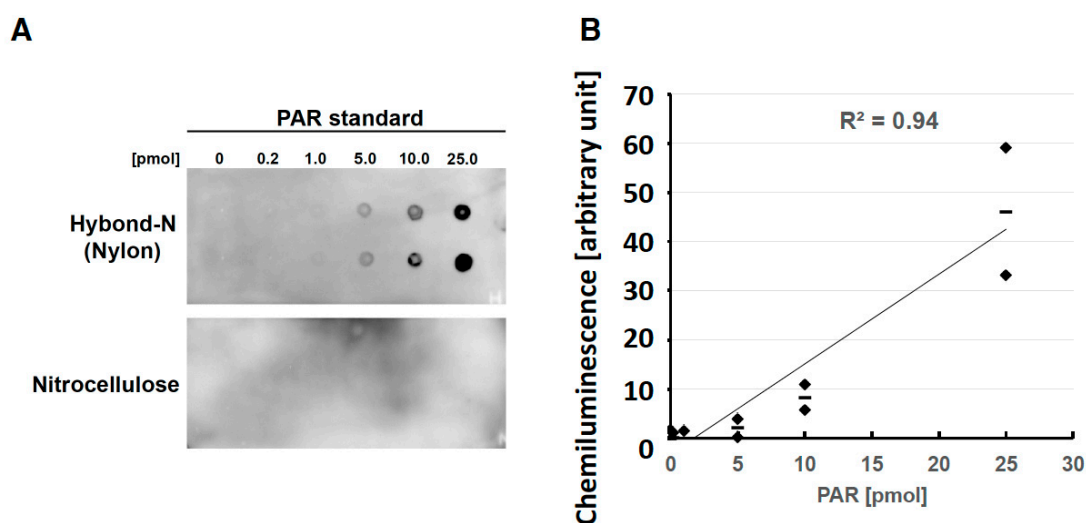


Figure 1. Comparison of Hybond-N and nitrocellulose for PAR level detection with dot blot assay. (A) Different amounts of PAR were similarly spotted in duplicate on Hybond-N (**upper panel**) and nitrocellulose (**lower panel**) and were subjected to immunoblotting with anti-PAR 10H antibody; (B) Plots for chemiluminescence detected with Hybond-N in (A). The bars indicate mean values.

For a slot blot assay of nucleic acids, chemical or physical crosslink methods are known to enhance the detection [14]. We therefore analyzed the effects of UV crosslink on PAR detection. As shown in Figure 2A,B, UV crosslink alone for 50 s at 254 nm ($120 \text{ mJ}/\text{cm}^2$) increased the detection intensity at least several folds. An increase in the detected level incline by UV crosslinking was observed as shown in Figure 2B, whereas the lower limit of detection was not improved. The detection sensitivity with a crosslink at 312 nm was slightly lower compared to that at 254 nm (data not shown).

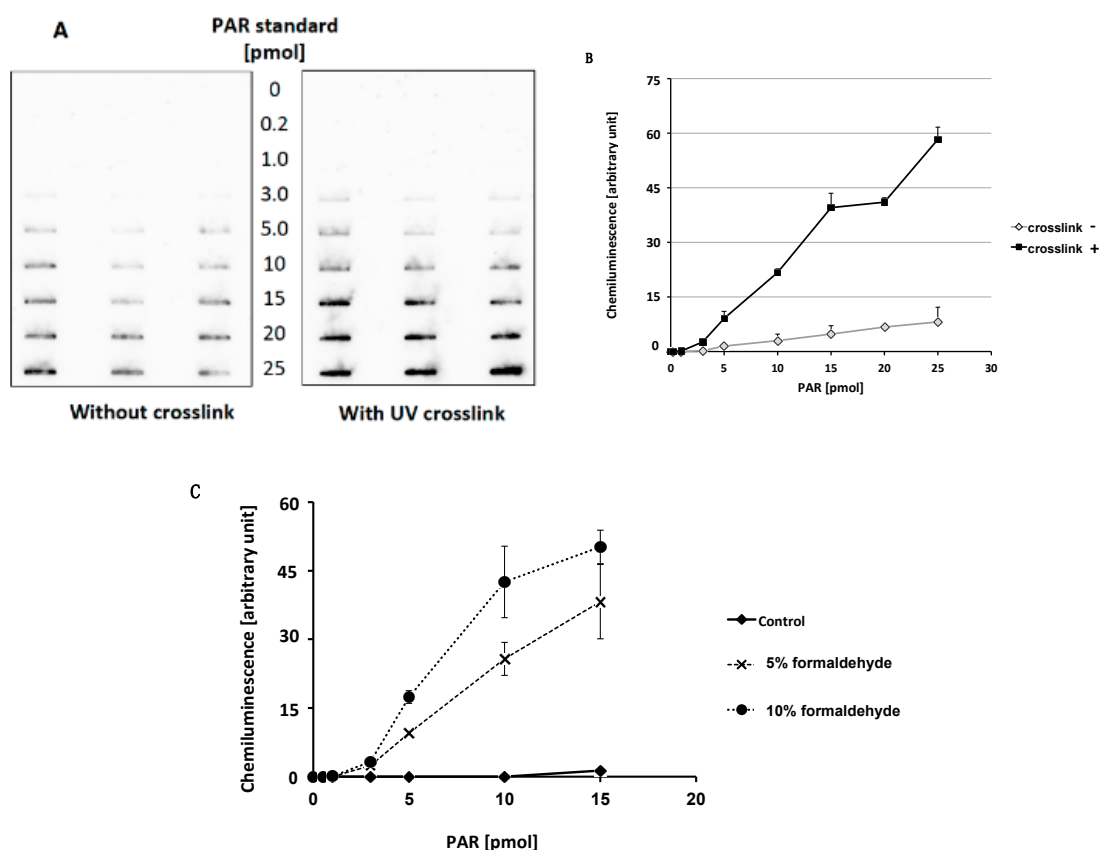


Figure 2. The effect of crosslinking for poly(ADP-ribose) (PAR) detection on Hybond-N. (A) Detected chemiluminescence on the membrane without and with UV crosslinking. PAR was spotted in triplicate and after drying, crosslinking was carried out at 254 nm; (B) Plot for the amount of PAR and the measured chemiluminescence without and with UV crosslinking at 120 mJ/cm²; (C) The effect of chemical crosslinking with formaldehyde solution for PAR detection on Hybond-N. The values, mean \pm SE.

We also examined the effect of a chemical crosslink with a formaldehyde solution. The incubation of a blotted membrane with 5% and 10% formaldehyde solutions at 37 °C for 20 min was examined. As shown in Figure 2C, when purified PAR was used without any additional components, 5% and 10% formaldehyde increased the detection level incline of PAR but did not increase the lower limit of detection. However, we found that in the presence of cellular components, crosslink with formaldehyde did not augment the detection levels of PAR (data not shown).

2.2. Effects of PAR Length on Detection with Slot Blot Assay of PAR

Next, we examined the relationship of PAR chain length and detection sensitivity with the UV crosslinking method. The prepared PAR fractions were QF, QC, and 60% QC, the mean chain length of which were around 26, 20, and 17 residues, respectively [15]. As shown in Figure 3, when these PAR fractions were subjected to the slot blot assay, the QF fraction showed a two-fold higher detection level compared to the QC fraction. On the other hand, the 60% QC fraction was not detected even at 10 pmol in ADP-ribose residues. This suggests that PAR shorter than 20 residues could not be detected in the slot blot assay even with the UV crosslinking method.

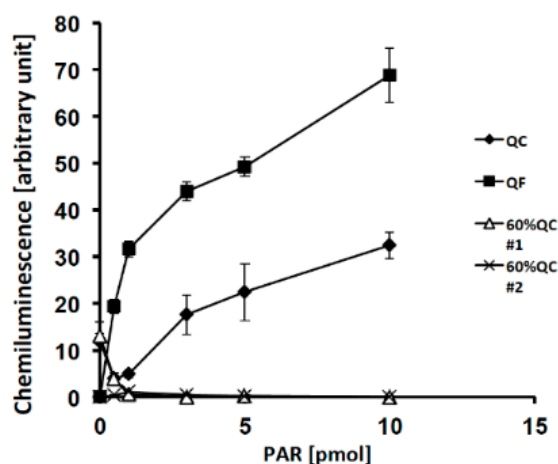


Figure 3. Effect of PAR length for detection by slot blot assay under UV crosslink conditions. A QC fraction, QF fraction, and 60% QC fraction were used as PAR samples, the mean chain length of which were around 26, 20, and 17 ADP-ribose residues, respectively [15]. The values, mean \pm SE.

2.3. Detection of PAR Level Changes with Slot Blot Assay in Cultured Cells

We further analyzed detection of endogenous PAR level in the cells. For this purpose, we used mouse ES cells of wild-type and *Parp-1*^{-/-} genotypes. When ES cells were treated with 0.3 mM MMS, we previously detected about 3–4-fold increase of the PAR level 1 and 5 h after the MMS treatment in *Parp-1*^{-/-} but not in wild-type ES cells after digestion of PAR into ADP-ribose and measurement with HPLC [16]. As shown in the slot blot assay of Figure 4, the PAR level in wild-type and *Parp-1*^{-/-} ES cells did not show any increase after the MMS treatment in the crude extract. The endogenous level of PAR in wild-type ES cells seems to be near the detection limit. The results suggest that if an endogenous PAR level in mouse ES cells and PBMCs are in a similar range, the endogenous PAR level of 2.0×10^4 PBMCs may be under the detection level in a slot blot assay even with the UV crosslink method.

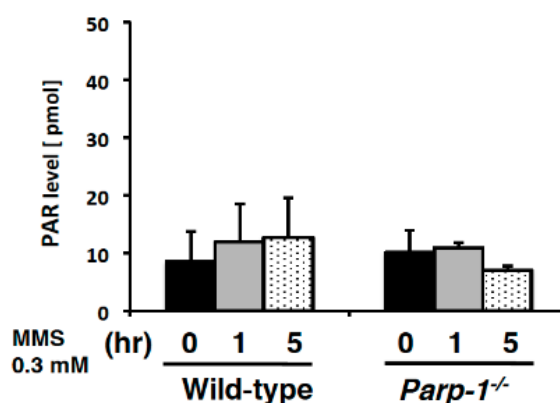


Figure 4. PAR level changes detected by slot blot assay in mouse ES cells after MMS treatment. The wild-type and *Parp-1*^{-/-} ES cells treated with 0.3 mM MMS and the cell crude extract were subjected to PAR level measurement 1 and 5 h after MMS addition with untreated controls. PAR levels from the inoculated 2.7×10^5 ES cells are shown. The bars, mean \pm SE. Statistical significances are not detected.

2.4. PAR Levels in Mouse PBMCs Detected with Ex Vivo PARP Assay

Next, PBMCs were prepared from C57BL/6J mice and subjected to PAR detection after an ex vivo PAR synthesis reaction. As shown in Figure 5A,B, without addition of the substrate NAD⁺

and activated DNA, the PAR level was less than 5 pmol ADP-ribose residues/6 min/ 2.0×10^4 cells. However, when 350 μM NAD^+ and 10 $\mu\text{g}/\text{mL}$ of activated DNA were added, namely with ex vivo PARP activity measurement conditions, increased incorporation of NAD into PAR was detected ($p < 0.05$). Three mice showed a similar level of PAR ($p = 0.587$) (Figure 5C). This level was slightly higher than the PAR level in human PBMCs, namely around 3 pmol ADP-ribose residues/6 min/ 2.0×10^4 cells detected, as reported by Plummer et al. with an ex vivo assay [6].

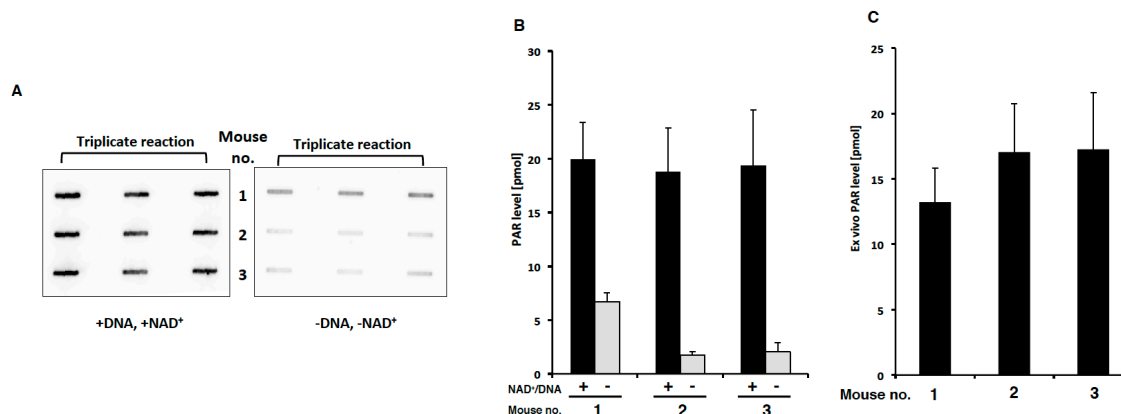


Figure 5. PAR levels in mouse PBMC detected in ex vivo assay with addition of 10 $\mu\text{g}/\text{mL}$ activated DNA and 350 μM NAD^+ . (A) Detected chemiluminescence on the membranes with UV crosslinking at 120 mJ/cm^2 . Triplicate samples were subjected to slot blot assay. PBMC from C57BL/6J male mice of 12–13 months old were used; (B) The plot of PAR level without and with NAD^+ /activated DNA. The addition of NAD^+ at 350 μM NAD^+ and activated DNA at 10 $\mu\text{g}/\text{mL}$ increased PAR level during ex vivo PAR synthesis reaction ($p < 0.05$); (C) The PAR level detected ex vivo (pmol ADP-ribose residues/6 min/ 2.0×10^4 cells) calculated from B. The bars, mean \pm SE.

When the clinically-used PARP inhibitor olaparib was intraperitoneally injected into C57BL/6J male mice of 7 weeks age at 50 mg/kg body weight, PAR levels in PBMCs showed a tendency to decrease to 40% at 8 h ($p = 0.127$ for the value of 8 h versus control) but recovered to the control level at 24 h ($p = 0.827$ for the value of 24 h versus control) after olaparib administration (Figure 6).

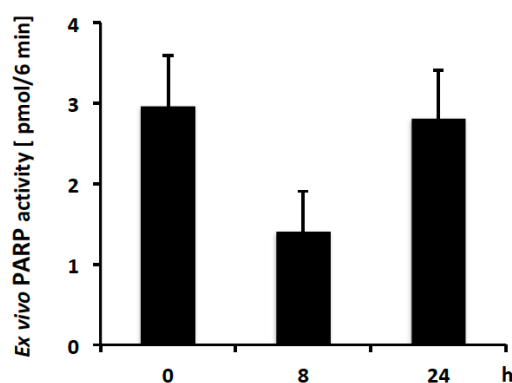


Figure 6. Changes in PAR ex vivo levels after i.p. injection of C57BL/6J male mice of 7 weeks old with olaparib at 50 mg/kg body weight. $n = 3$. The ex vivo PAR levels, measured in the presence of NAD^+ , and DNA subtracted by the PAR level, measured in the absence of NAD^+ and DNA, are shown. The bars, mean \pm SE. A tendency to decrease at 8 h ($p = 0.127$ for the value of 8 h versus control) of the PAR level was observed after olaparib administration. UV crosslink condition was used.

3. Discussion

In this study, we investigated the optimum condition for PAR detection with a slot blot assay of PAR. We showed that the use of a nylon membrane and UV crosslink at 254 nm could stably enhance the detection level. A poor retention of free DNA on membranes was previously reported to be improved by covalent cross-linking upon UV irradiation by Kalachikov et al. [14]. However, the PAR with less than 20 ADP-ribose residues cannot be detected even with the UV crosslinking method. It has been reported that 10H antibody can bind PAR of more than 20 residues but not shorter [5], so the properties of 10H antibody are likely to limit the detection of PAR less than 20 residues in length. PAR synthesis reaction by PARP1 is known to produce branched PAR chains [17]. Although the frequencies of branches are suggested to be low at around 10% or less in a typical *in vitro* reaction by PARP1, the detection level of branched chains should also be clarified in future studies.

Various methods are reported for the measurement of the PAR and PARP inhibition levels. Sandwich ELISA methods using anti-PAR antibodies have been reported [18], and the detection limit was around 9 fmol as ADP-ribose residues (5 pg) [19]. The NCI-advised protocol for a PD assay for a PARP inhibitor intends to detect endogenous PAR levels, for example with 10^7 cells of PBMCs [13]. An improved PD assay for a PARP inhibitor has further been reported that utilizes an enhancement method by gamma ray-irradiation of PBMCs at 8 Gy and incubation on ice for 1 h before an *ex vivo* assay [20]. With this method, PAR detection level increased to around 107 pg/ 10^7 cells, namely around 20-fold. However, if the ELISA method uses a 10H antibody as a capture or detection antibody, PAR less than 20 residues in length could not be detected, which thus limits the accuracy of the detection level.

In the current study and ELISA method, the standard PAR molecules used are protein-free PAR. It would be best to obtain the quantified protein-bound PAR with a controlled length as a standard for the slot blot assay and ELISA. However, it is hard to obtain the protein-bound PAR with controlled length as standard. Therefore, when protein-free PAR is used as a standard, the slot blot assay or ELISA method for measurement of PAR could not be fully accurate but remains as semi-quantitative.

The PD assay carried out by Plummer et al. uses PBMCs isolated from the blood of patients treated with PARP inhibitors [6], and in a subsequent *ex vivo* assay, the inhibition of PAR synthesis seemed to be stably detected, possibly because the tight trapping of PARP inhibitors to PARP1 molecules was maintained [21].

In the current study, the improvement of the slot blot PARP activity assay by a combination of the use of a nylon membrane and the UV cross-linking method for the cell lysates of PBMCs has been investigated. PAR detection using an antibody to PAR was initially reported by Affar et al. [22]. The use of a nylon membrane for a dot blot assay of *ex vivo* PAR levels with 10,000 cells and 1 mM NAD⁺ and oligodeoxynucleotides of 8 residues as activators was previously reported by Pfeiffer et al. [23]. The positively-charged membrane Hybond-N⁺ was also reported to enhance the detection level of PAR compared with that of a nylon membrane [24].

The further optimization of PAR detection applicable to a PD assay for a PARP inhibitor and crude sample measurement should also be studied to establish the measurement method of endogenous PARP activity. The detection of PAR with short (mono to several residues) chain length and branched chains could also be the issue for further study, although the method with PAR digestion to ADP-ribose with PARG and subsequent analysis with HPLC as ADP-ribose residues has been used for the detection of PAR [16], and the PAR digestion with phosphodiesterase and detection as phosphoribosyl phosphate has been also effectively used [25].

Additionally, for an optimized PD assay, studies to detect PARP activity levels with cancer cells less than 10^3 – 10^5 cells, obtained from biopsy, surgery, or circulating tumor cells [26], and PBMCs would be necessary for the precise monitoring of PARP inhibition levels. Because PAR is easily degraded in the presence of blood components [27], an *ex vivo* assay system should contain a minimum level of contaminated blood components.

The merit of the slot blot assay for PAR detection may also be in its feasibility and low costs. Compared with ELISA, the lower sensitivity limit should be approximately 500-fold higher, and the

upper limit of detection could be as high as around 25 pmol of ADP-ribose residues with a slot blot assay. This detection range of a slot blot assay could be useful to analyze crude samples with an unknown range of PAR levels, not only for a PD assay of PARP inhibitors but also for the measurement of PARP activity in various types of crude samples from the environment.

4. Materials and Methods

4.1. Preparation of PAR Using Recombinant PARP-1

PAR was prepared using recombinant PARP-1 expressed in *E. coli*, and the crude extract was used for the PAR synthesis reaction [15]. PAR was prepared as previously described using the steps of phenol precipitation, elution from anion-exchange column (Qiagen-tip500, Qiagen, Hilden, Germany), dialysis, and lyophilization. Prepared PAR fractions were QF, QC, and 60% QC, with a mean chain length of each around 26, 20, and 17 residues, respectively [15].

4.2. Slot Bot Assay of PAR

PAR was manually spotted on nitrocellulose (GE Healthcare, Little Chalfont, UK), a nylon membrane (Hybond-N, GE Healthcare), or using MINIFOLD II (Schleicher & Schuell, Dassel, Germany) as slots. The membranes were then dried and soaked into $1 \times$ Tris-buffered saline (TBS)/0.1% Tween20 (TBST) and transferred to a blocking solution consisting of 5% skim milk, $1 \times$ PBS/0.1% Tween20 (PBS-MT) for 1 h at room temperature. The membrane was then incubated with the 1st antibody anti-PAR 10H (1:1000, Enzo Biochem Inc., New York, NY, USA) overnight at 4 °C. The second antibody incubation was carried out with anti-mouse IgG (1:1000, GE Healthcare) for 1 h at room temperature, and detection of the signals was carried out with Immobilon Western Chemiluminescent HRP Substrate (Millipore, Burlington, VT, USA) or SuperSignal West Femto Maximum Sensitivity Substrate (Thermo Fisher Scientific, Waltham, MA, USA), and the relative level of chemiluminescence was quantified with LAS-3000 or LAS-1000 (FUJI FILM, Tokyo, Japan).

4.3. Ex Vivo Assay of PARP Activity

Ex vivo PARP activity was measured as previously reported by Plummer et al. [6] with some modifications. Briefly, frozen mouse PBMCs were thawed and suspended on ice with 50 μ L of 0.15 mg/mL digitonin (Sigma-Aldrich, St. Louis, MO, USA) and the proteinase inhibitor cocktail Complete (Roche, Basel, Switzerland) and stood on ice for 5 min. 450 μ L of isotonic buffer consisting of 7 mM HEPES-buffer (pH 7.8), 26 mM potassium chloride, 0.1 mM dextran, 0.4 mM EGTA, 0.5 mM $MgCl_2$, and 45 mM sucrose was added, and the number of nuclei was counted. A cell suspension of 2.0×10^4 cells was then adjusted to a 100 μ L mixture containing 100 mM Tris-HCl (pH 7.8), 12 mM $MgCl_2$, 1 mM dithiothreitol, 10 μ g/mL activated DNA (Sigma D4522, calf thymus DNA partially digested with DNase), and 350 μ M NAD^+ . The PAR synthesis reaction was carried out for 6 min at 26 °C with shaking and stopped with the addition of 400 μ L of 12.5 μ M olaparib (Selleckchem, Houston, TX, USA) as described [6].

4.4. Extraction of PBMC from Mice

C57BL/6J male mice (7 months old, Clea Japan, Fujinomiya, Japan) were intraperitoneally injected with 50 mg/kg body weight of olaparib (Selleckchem), prepared in 10% dimethylsulfoxide in PBS(-)/10% 2-hydroxypropyl- β -cyclodextrin as reported [28], and 8 and 24 h after injection, blood was taken into heparin-coated syringes, and volumes were adjusted to 3 mL with saline. In other experiments, C57BL/6J male mice of 12–13 months old were used. PBMCs were isolated using Accuspin (Sigma-Aldrich). After centrifuging at $1000 \times g$ for 10 min, the PBMC layer was transferred to a tube, and after rinsing twice with 5 mL of ice-cold PBS(-), PBMCs were transferred with 2 mL of PBS(-) into new tubes, and after removing supernatant, they were snap-frozen with liquid nitrogen and stored at 80 °C until use. The mouse experiments were approved by the Animal Experimental Committee of

the National Cancer Center and performed following the Guidelines for Animal Experiments of the National Cancer Center, which meet the ethical guidelines for experimental animals in Japan.

4.5. UV Crosslinking

PAR was blotted onto nylon or nitrocellulose membranes, and after drying the membrane, UV irradiation was carried out with a UV Stratalinker 2400 (Stratagene, La Jolla, CA, USA) at 254 nm for 50 s or longer at 120 mJ/cm². A UV transilluminator (Atto, Tokyo, Japan) was also used for crosslinking at 312 nm for 30–180 s. After UV crosslinking, the membrane was incubated with the 1st antibody (anti-PAR antibody) and the 2nd antibody, and it was processed for the detection of chemiluminescence. For the ex vivo assay of PARP activity, the reaction mixture was transferred onto the membrane, dried, and then UV crosslinking was carried out.

4.6. Chemical Crosslinking

PAR blotted membranes were dried as above, incubated in 5% or 10% formaldehyde solution at 37 °C for 20 min, and then incubated with TBS for 2 min twice. After drying, the membrane was incubated with the 1st antibody (anti-PAR antibody) and 2nd antibody, and then it was processed for detection of chemiluminescence. After blotting of PAR onto the membranes and drying, the membranes were incubated with formaldehyde solution and dried again. The membrane was then crosslinked with UV irradiation and processed with antibodies for detection as above.

4.7. Culture of Mouse Wild-Type ES Cells

Parp-1^{-/-} and parental wild-type J1 ES cells [29,30] were cultured in undifferentiated condition in the presence of a leukemia inhibitory factor, as previously described. The amount of 1 × 10⁶ cells were inoculated in 6 well plates in triplicate, and they were treated with an alkylating agent, methylmethanesulfonate (MMS), at 0.3 mM for 1 and 5 h to induce PAR synthesis. The crude extract was prepared by the addition of 300 µL of an extraction buffer consisting of 10 mM Tris-HCl (pH 7.4), 10 mM EDTA, 0.5% Triton X-100, and sonication for 5 s three times in ice-water. Centrifugation was then carried out at 17,000 × g for 10 min at 4 °C to obtain the supernatant fraction. Eighty µL of the sample was spotted on the slot blot manifold.

4.8. Statistical Analysis

Statistical analysis was performed using the Mann-Whitney *U* test using JMP (SAS Institute Inc., Cary, NC, USA) software.

Author Contributions: M.M., J.H., M.W., T.N., and K.T. conceived and designed the experiments; UK. Y.S., and M.M. performed the experiments; Y.K., Y.S., T.O., M.M., and T.N. analyzed the data; M.M., Y.K., Y.S., M.W., and T.O. wrote the paper.

Funding: This research is partially supported by The Practical Research for Innovative Cancer Control from Japan Agency for Medical Research and Development, Japan Agency for Medical Research and Development (15Ack0106021, 17Ik0201048h0002), and Grant-in-Aid for Scientific Research (KibanB 22300343, H23-Jitsuyoka(Gan)-004) to M.M.

Acknowledgments: We thank Masayoshi Takagi for giving kind advice and supports for this study.

Conflicts of Interest: The authors declare no conflicts of interest.

References

1. Schreiber, V.; Dantzer, F.; Ame, J.C.; de Murcia, G. Poly(ADP-ribose): Novel functions for an old molecule. *Nat. Rev. Mol. Cell Biol.* **2006**, *7*, 517–528. [[CrossRef](#)] [[PubMed](#)]
2. Kanai, Y.; Kawaminami, Y.; Miwa, M.; Matsushima, T.; Sugimura, T. Naturally-occurring antibodies to poly(ADP-ribose) in patients with systemic lupus erythematosus. *Nature* **1977**, *265*, 175–177. [[CrossRef](#)] [[PubMed](#)]

3. Kanai, Y.; Sugimura, T. Comparative studies on antibodies to poly(adp-ribose) in rabbits and patients with systemic lupus erythematosus. *Immunology* **1981**, *43*, 101–110. [[PubMed](#)]
4. Kanai, Y. Overview on poly(adp-ribose) immuno-biomedicine and future prospects. *Proc. Jpn. Acad. Ser. B Phys. Biol. Sci.* **2016**, *92*, 222–236. [[CrossRef](#)] [[PubMed](#)]
5. Kawamitsu, H.; Hoshino, H.; Okada, H.; Miwa, M.; Momoi, H.; Sugimura, T. Monoclonal antibodies to poly (adenosine diphosphate ribose) recognize different structures. *Biochemistry* **1984**, *23*, 3771–3777. [[CrossRef](#)] [[PubMed](#)]
6. Plummer, E.R.; Middleton, M.R.; Jones, C.; Olsen, A.; Hickson, I.; McHugh, P.; Margison, G.P.; McGown, G.; Thorncroft, M.; Watson, A.J.; et al. Temozolomide pharmacodynamics in patients with metastatic melanoma: Dna damage and activity of repair enzymes o6-alkylguanine alkyltransferase and poly(adp-ribose) polymerase-1. *Clin. Cancer Res.* **2005**, *11*, 3402–3409. [[CrossRef](#)] [[PubMed](#)]
7. Curtin, N.J. Parp inhibitors for cancer therapy. *Expert Rev. Mol. Med.* **2005**, *7*, 1–20. [[CrossRef](#)] [[PubMed](#)]
8. Sisay, M.; Edessa, D. Parp inhibitors as potential therapeutic agents for various cancers: Focus on niraparib and its first global approval for maintenance therapy of gynecologic cancers. *Gynecol. Oncol. Res. Pract.* **2017**, *4*, 18. [[CrossRef](#)] [[PubMed](#)]
9. Bryant, H.E.; Schultz, N.; Thomas, H.D.; Parker, K.M.; Flower, D.; Lopez, E.; Kyle, S.; Meuth, M.; Curtin, N.J.; Helleday, T. Specific killing of brca2-deficient tumours with inhibitors of poly(adp-ribose) polymerase. *Nature* **2005**, *434*, 913–917. [[CrossRef](#)] [[PubMed](#)]
10. Farmer, H.; McCabe, N.; Lord, C.J.; Tutt, A.N.; Johnson, D.A.; Richardson, T.B.; Santarosa, M.; Dillon, K.J.; Hickson, I.; Knights, C.; et al. Targeting the DNA repair defect in brca mutant cells as a therapeutic strategy. *Nature* **2005**, *434*, 917–921. [[CrossRef](#)] [[PubMed](#)]
11. McCabe, N.; Turner, N.C.; Lord, C.J.; Kluzek, K.; Bialkowska, A.; Swift, S.; Giavara, S.; O'Connor, M.J.; Tutt, A.N.; Zdzienicka, M.Z.; et al. Deficiency in the repair of DNA damage by homologous recombination and sensitivity to poly(adp-ribose) polymerase inhibition. *Cancer Res.* **2006**, *66*, 8109–8115. [[CrossRef](#)] [[PubMed](#)]
12. Wang, J.; Ding, Q.; Fujimori, H.; Motegi, A.; Miki, Y.; Masutani, M. Loss of ctip disturbs homologous recombination repair and sensitizes breast cancer cells to parp inhibitors. *Oncotarget* **2016**, *7*, 7701–7714. [[CrossRef](#)] [[PubMed](#)]
13. N.D.C. Available online: <http://dctd.Cancer.Gov/researchresources/biomarkers/polyadenosylribose.htm> (accessed on 20 June 2018).
14. Kalachikov, S.M.; Adarichev, B.A.; Dymshits, G.M. Immobilization of DNA on microporous membranes using uv-irradiation. *Bioorg. Khim.* **1992**, *18*, 52–62. [[PubMed](#)]
15. Shimokawa, T.; Ogino, H.; Maeda, D.; Nakagama, H.; Sugimura, T.; Masutani, M. Poly(adp-ribose) preparation using anion-exchange column chromatography. *Org. Chem. Insights* **2009**, *2*, 1–5.
16. Shirai, H.; Poetsch, A.R.; Gunji, A.; Maeda, D.; Fujimori, H.; Fujihara, H.; Yoshida, T.; Ogino, H.; Masutani, M. Parg dysfunction enhances DNA double strand break formation in s-phase after alkylation DNA damage and augments different cell death pathways. *Cell Death Dis.* **2013**, *4*, e656. [[CrossRef](#)] [[PubMed](#)]
17. Miwa, M.; Saikawa, N.; Yamaizumi, Z.; Nishimura, S.; Sugimura, T. Structure of poly(adenosine diphosphate ribose): Identification of 2'-[1''-ribose]-2''-(or 3''-)(1'''-riboseyl)adenosine-5',5'',5'''-tris(phosphate) as a branch linkage. *Proc. Natl. Acad. Sci. USA* **1979**, *76*, 595–599. [[CrossRef](#)] [[PubMed](#)]
18. Veskimae, K.; Staff, S.; Gronholm, A.; Pesu, M.; Laaksonen, M.; Nykter, M.; Isola, J.; Maenpaa, J. Assessment of parp protein expression in epithelial ovarian cancer by elisa pharmacodynamic assay and immunohistochemistry. *Tumour Biol.* **2016**, *37*, 11991–11999. [[CrossRef](#)] [[PubMed](#)]
19. Ida, C.; Yamashita, S.; Tsukada, M.; Sato, T.; Eguchi, T.; Tanaka, M.; Ogata, S.; Fujii, T.; Nishi, Y.; Ikegami, S.; et al. An enzyme-linked immunosorbent assay-based system for determining the physiological level of poly(adp-ribose) in cultured cells. *Anal. Biochem.* **2016**, *494*, 76–81. [[CrossRef](#)] [[PubMed](#)]
20. De Haan, R.; Pluim, D.; van Triest, B.; van den Heuvel, M.; Peulen, H.; van Berlo, D.; George, J.; Verheij, M.; Schellens, J.H.M.; Vens, C. Improved pharmacodynamic (pd) assessment of low dose parp inhibitor pd activity for radiotherapy and chemotherapy combination trials. *Radiother. Oncol.* **2017**, *126*, 443–449. [[CrossRef](#)] [[PubMed](#)]
21. Murai, J.; Huang, S.Y.; Das, B.B.; Renaud, A.; Zhang, Y.; Doroshow, J.H.; Ji, J.; Takeda, S.; Pommier, Y. Trapping of parp1 and parp2 by clinical parp inhibitors. *Cancer Res.* **2012**, *72*, 5588–5599. [[CrossRef](#)] [[PubMed](#)]

22. Affar, E.B.; Duriez, P.J.; Shah, R.G.; Sallmann, F.R.; Bourassa, S.; Kupper, J.H.; Burkle, A.; Poirier, G.G. Immunodot blot method for the detection of poly(adp-ribose) synthesized in vitro and in vivo. *Anal. Biochem.* **1998**, *259*, 280–283. [[CrossRef](#)] [[PubMed](#)]
23. Pfeiffer, R.; Brabeck, C.; Burkle, A. Quantitative nonisotopic immuno-dot-blot method for the assessment of cellular poly(adp-ribosyl) ation capacity. *Anal. Biochem.* **1999**, *275*, 118–122. [[CrossRef](#)] [[PubMed](#)]
24. Beneke, S.; Scherr, A.L.; Ponath, V.; Popp, O.; Burkle, A. Enzyme characteristics of recombinant poly(adp-ribose) polymerases-1 of rat and human origin mirror the correlation between cellular poly(adp-ribosyl) ation capacity and species-specific life span. *Mech. Ageing Dev.* **2010**, *131*, 366–369. [[CrossRef](#)] [[PubMed](#)]
25. Zubel, T.; Martello, R.; Burkle, A.; Mangerich, A. Quantitation of poly(adp-ribose) by isotope dilution mass spectrometry. *Methods Mol. Biol.* **2017**, *1608*, 3–18. [[PubMed](#)]
26. Burinaru, T.A.; Avram, M.; Avram, A.; Marculescu, C.; Tincu, B.; Tucureanu, V.; Matei, A.; Militaru, M. Detection of circulating tumor cells using microfluidics. *ACS Comb. Sci.* **2018**, *20*, 107–126. [[CrossRef](#)] [[PubMed](#)]
27. Okajima, Y.; Yoshida, T.; Fujimori, H.; Wang, J.; Harada, H.; Suzuki, Y.; Suzuki, H.; Masutani, M. Rapid degradation of poly(adp-ribose) after injection into the mouse bloodstream. *Biol. Pharm. Bull.* **2013**, *36*, 462–466. [[CrossRef](#)] [[PubMed](#)]
28. Senra, J.M.; Telfer, B.A.; Cherry, K.E.; McCrudden, C.M.; Hirst, D.G.; O'Connor, M.J.; Wedge, S.R.; Stratford, I.J. Inhibition of parp-1 by olaparib (azd2281) increases the radiosensitivity of a lung tumor xenograft. *Mol. Cancer Ther.* **2011**, *10*, 1949–1958. [[CrossRef](#)] [[PubMed](#)]
29. Fujihara, H.; Ogino, H.; Maeda, D.; Shirai, H.; Nozaki, T.; Kamada, N.; Jishage, K.; Tanuma, S.; Takato, T.; Ochiya, T.; et al. Poly(Adp-ribose) Glycohydrolase Deficiency Sensitizes mouse ES Cells to DNA Damaging Agents. *Curr. Cancer Drug Targets* **2009**, *9*, 953–962. [[CrossRef](#)] [[PubMed](#)]
30. Nozaki, T.; Masutani, M.; Watanabe, M.; Ochiya, T.; Hasegawa, F.; Nakagama, H.; Suzuki, H.; Sugimura, T. Syncytiotrophoblastic giant cells in teratocarcinoma-like tumors derived from parp-disrupted mouse embryonic stem cells. *Proc. Natl. Acad. Sci. USA* **1999**, *96*, 13345–13350. [[CrossRef](#)] [[PubMed](#)]



© 2018 by the authors. Licensee MDPI, Basel, Switzerland. This article is an open access article distributed under the terms and conditions of the Creative Commons Attribution (CC BY) license (<http://creativecommons.org/licenses/by/4.0/>).